Supramolecular gels of cholesterol-modified gellan gum with disc-like and worm-like micelles

Nicole Zoratto[1,3], Isabelle Grillo[2,‡], Pietro Matricardi[3], Cécile A. Dreiss[1]

[1]Institute of Pharmaceutical Science, King's College London, 150 Stamford Street, London SE1 9NH, UK

[2]Institut Laue Langevin, 71 avenue des martyrs, B.P. 156, 38042 Grenoble Cedex 9, France

[3]Department of Drug Chemistry and Technologies, "Sapienza" University of Rome, Rome, Italy

Abstract

The association between a hydrophobically modified polysaccharide, gellan gum, with micelles based on a surfactant bearing the same hydrophobic tail as pendant groups was investigated by rheology and small-angle neutron scattering (SANS). Gellan gum grafted with cholesterol groups (20% mol/mol tetrasaccharide unit), GeCh, was mixed with polyoxyethylene cholesteryl ether ($ChEO_{10}$), which comprises a cholesterol group as the tail linked to a small polyoxyethylene headgroup, and self-assembles into micelles with an unusual disc-like morphology. The addition of 0.5% polymer to solutions of $ChEO_{10}$ induced a remarkable transition from a Newtonian fluid to a predominantly solid-like viscoelastic behaviour, leading to a $\times 10^5$ increase in zero-shear viscosity (with 5% $ChEO_{10}$). Increasing surfactant concentration led to an enhancement of the viscoelasticity, but the elastic modulus *G'* reached a plateau around 15% surfactant, attributed to a saturation of the sticker groups. The effect of micellar morphology on the network was studied by adding a small headgroup co-surfactant, triethylene glycol monododecyl ether, to $ChEO_{10}$ micelles, which drives their elongation into wormlike micelles. Networks obtained with the long, flexible micelles displayed enhanced solid-like behaviour, with no cross-over between *G'* and *G"* over the measured range of frequencies, reflecting relaxation times of the order of minutes or hours. The morphology of the gels studied by SANS revealed a scattering dominated by strongly interacting micelles (described by discs of 140 Å diameter and a hydrated ~38 Å PEO corona) and the presence of micellar clusters induced by the presence of the polymer. The scattering data therefore confirm that the onset of gelation is due to surfactant micelles acting as junction points for the network.

Keywords: hydrophobically modified polymers, supramolecular gels, associative networks, polyoxyethylene cholesteryl ether, small-angle neutron scattering, wormlike micelles, oscillatory rheology

Introduction

‡ As revisions of this manuscript were being prepared, our long-term colleague, ILL staff scientist, Isabelle Grillo tragically passed away. We wish to dedicate this manuscript to her memory.

While chemical crosslinking has traditionally been used to build three-dimensional polymer networks, there has been a growing interest over the last couple of decades to build supramolecular hydrogels from non-covalent interactions, through host-guest complexation, hydrogen bonds, electrostatic or hydrophobic interactions [1-3]. The reversible nature of the interactions leads to a range of advantageous characteristics, including responsiveness, easy tailoring of dynamic properties, shear-thinning and thus properties such as injectability or self-healing, which make these gels more suited towards biomedical applications than the more traditional chemically cross-linked gels. Obviously, the biocompatibility of the starting materials is key to the final characteristics of the hydrogels and its translation into functional materials. This, added to the drive towards renewable resources, has placed a strong emphasis on using building blocks from natural sources. In this work, we propose a simple strategy based on the synergistic association of surfactants with a hydrophobically modified biopolymer, gellan gum, where the pendant groups share the same chemical nature (steroid motif) as the surfactant hydrophobic tails.

Hydrophobically modified polymers (HMP) are water-soluble polymers onto which strongly hydrophobic residues are chemically attached, either to both ends [4-6] or, more commonly, along the hydrophilic polymer backbone [7-9]. The presence of these hydrophobic groups imparts the polymer the capability to self-assemble, forming either networks [10, 11] or suspensions [12, 13], and to associate with other molecules presenting hydrophobic groups; they are, for this reason, also referred to as "associative polymers". The spontaneous association of HMP with additives such as surfactants usually induces the formation of networks where the hydrophobic domains act as junction points, drastically affecting the solution dynamics. Mixtures of HMP and surfactants have been studied extensively both because of their industrial relevance, as they are present in many commercial and technological products, such as paints, coatings, fracturing fluids [7, 9, 10, 14], also more recently in the pharmaceutical and biomedical fields [15, 16, 17, 18]; they also are intriguing systems with complex dynamics and topologies, which are of notable interest from a fundamental perspective [19, 11, 12]. The vast majority of studies have explored the association of polymers with either low concentrations of surfactant, or 'conventional' micelles (small, spherical) [20], while mixtures of HMP with elongated micelles, or wormlike micelles (WLM), has been much less explored [13, 10, 5, 21, 18]. WLM are elongated and semi-flexible aggregates of surfactants [22, 23], which, similarly to polymers, entangle with each other above a critical overlap concentration, C^*, forming a transient network characterized by a predominantly solid-like viscoelastic rheological response. However, the reversibility of the aggregation process differentiates them from conventional polymers: WLM constantly break and reform in a dynamic equilibrium, making them "living polymers". The association of HMP with WLM usually leads to an enhancement of the viscoelastic properties, which are not achievable with the individual components [13, 18]. The interaction of the polymer sticker groups with WLM cores can lead to different topologies, which dictates the dominant relaxation mechanisms [6]: the stickers may intercalate into the WLMs, forming a network that relaxes at long times due to sticker pullout [24], sometimes even strengthening the WLM network [10]; or, the polymer may be cross-linked by the surfactant, inducing a break-up of the WLMs into shorter cylindrical (or spherical) micelles in order to shield the stickers from the aqueous phase [13]. Comparing the networks built between HMP and

small or long (rod-like or worm-like) micelles, it is expected that long micelles may interact with the hydrophobes on a large number of adjacent chains, and, having also much longer micellar lifetimes, will lead to longer junction lifetimes and therefore larger relaxation times [11, 13, 25].

We have previously reported the associative networks formed between dextran modified with pendant cholesterol groups and either long or short micelles formed by the non-ionic, cholesterol-based surfactant, polyoxyethylene cholesteryl ether, $ChEO_{10}$ (**Figure 1**) [13]. Our results showed a strong synergistic behaviour, resulting from the hydrophobic interactions between the micellar cholesterol cores and the cholesterol pendant groups of the polymer backbone. Structural information obtained from small-angle neutron scattering (SANS) measurements revealed a very similar network for both systems, with the scattering signal dominated by the micelles. The addition of the polymer to viscoelastic WLM induced their break-up into smaller rods, therefore giving overall a response not too dissimilar to the smaller micelles, with however a wider spectrum of relaxation processes.

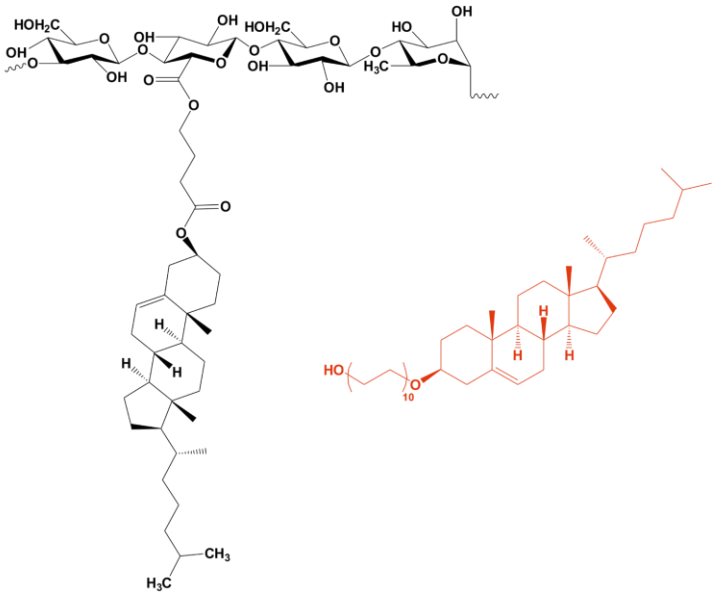

Figure 1. Repeating unit of the modified gellan gum (GeCh, black) and structure of the surfactant polyoxyethylene cholesteryl ether ($ChEO_{10}$, red).

This work explores the association of another hydrophobically modified biopolymer, gellan gum, with the same cholesterol-based surfactant, $ChEO_{10}$. Gellan gum (**Figure 1**) is a natural exopolysaccharide, FDA-approved food additive, with a widespread use in the food industry, and increasing interest in pharmaceutical technology due to its ability to form gels and nanoparticles [26-28]. At high temperatures, gellan gum is in its coil form, but undergoes a thermally-reversible transition from coil to double-helix at low temperatures; the further self-assembly of these anti-parallel double helices act as junction points for a three-dimensional physical network [29]. The advantageous properties of this biopolymer, such as biodegradability [30], non-toxicity [31], and ability to gel in the presence of cations [32], make it a useful excipient in multi-component

formulations for drug delivery through the oral, ophthalmic, and nasal routes [33] and for tissue engineering applications [34-36].

In this study, gellan gum was modified by grafting cholesterol pendant groups along its backbone, the starting point of self-assembled nanohydrogels developed in our group [28]. Its association with either *short* ($ChEO_{10}$) or *long* micelles was then explored, where the *long* (wormlike) micelles are obtained by mixing $ChEO_{10}$ with small amounts of the small headgroup co-surfactant triethylene glycol monododecyl ether, $C_{12}EO_3$. Compared to the previous study [13], very low concentrations of polymer are used (0.2 - 0.5 wt%) to induce the formation of three-dimensional networks, which are driven by cholesterol-cholesterol associations. The gels obtained from this interaction are characterized by oscillatory rheology over a wide range of surfactant concentrations (up to 20 wt%) and the underlying morphology is characterized by small-angle neutron scattering.

Experimental

Materials

Polyoxyethylene cholesteryl ether ($ChEO_{10}$, **Figure 1**) was purchased from Ikeda Corporation, Yokohama, Japan. Triethylene glycol monododecyl ether co-surfactant ($C_{12}EO_3$) (<98%), was obtained from Sigma-Aldrich Chemical Co. Ltd., UK. Gellan gum tetrabutylammonium salt (GeTBA, $M_w = 2.5\times10^5$ according to the supplier) were kindly provided by NOVAGENIT, Trento, Italy. Cholesterol (Ch), 4-bromobutyric acid, N-methyl-2-pyrrolidone. (NMP), N-(3-dimethylaminopropyl)-N'-ethylcarbodimide hydrochloride (EDC·HCl), 4-(dimethylamino)pyridine (DMAP), N-hydroxysuccinimide (NHS), tetramethylammonium chloride (TMA^+Cl^-), tetrabutylammonium bromide (TBA^+Br^-) were all obtained from Sigma. All solutions of surfactant, polymer and their mixture were prepared in D_2O (99% purity, Sigma Chemical Co.UK). All chemicals were used as received unless otherwise stated.

Modification of gellan gum with cholesterol

Ge-TBA underwent a controlled depolymerisation through extrusion (M-110EH-30 Microfluidizer® Processor). In detail, a solution of Ge-TBA (0.5% w/w) in water was prepared, then the resulting solution was forced to pass through a "Y" shaped extrusion chamber (G10Z, diameter 87 μm). The extrusion process was carried out at 1200 bar and the temperature of the solution was kept constant at 50°C during all steps. Seven extrusion cycles were performed on Ge-TBA solution. The measured intrinsic viscosity of the polymer was $[\eta] = 3.35$ dL/g and the overlap concentration, C^*, was estimated at 1.2%.

The synthesis of gellan cholesterol derivative is a two-step procedure, as described in references [28, 37]. Briefly, cholesterol was derivatized with 4-bromo-butyric acid, leading to the Br-butyric cholesterol (Ch-Br) derivative. Depolymerised Ge-TBA (200 mg, corresponding to 225 μmol of COOH groups) were dissolved in 16 mL of NMP. The Ch-Br derivative (24 mg), previously dissolved in 4-5 mL of NMP, was then added in order to obtain a Ge-TBA derivatization degree of 20% $mol \cdot mol^{-1}$ (mol of cholesterol per mol of Ge-TBA repeating units). The reaction was left to stir for 40 h at 38°C. An exhaustive dialysis against distilled water

was then carried out on the product (Visking tubing, cut-off: 12 000 - 14 000), until the conductivity of the solution was below 2 µS and GeCh was finally recovered by freeze-drying (yield: 90%). The derivatization degree was assessed by ^{1}H-NMR spectroscopy (400 MHz, Bruker Avance 400 spectrometer), performed in DMSO-d_6 at 27°C. The structure of the modified gellan, GeCh, is shown in **Figure 1**. GPC measurements of Ge and GeCh (tetrabutylammonium salt forms), were carried out in DMSO, using two serial columns (Phenogel 5 µm, 300 × 7.50 mm and 10^5 Å) at 60°C (flow rate: 0.6 mL/min) using a Viscotek Triple Detector Array (TDA) incorporating a Refractive Index (RI), Light Scattering and Viscosity detectors. DMSO was used as a common solvent for both Ge and GeCh. Detectors calibration was obtained by using pullulan (105×10^3) as a narrow standard, and dextran (73×10^3) as a broad standard. Each sample was filtered through a 0.22 µm syringe filter prior to analysis, and then injected at different concentrations (from 1 to 4 mg/mL) in order to obtain the proper refractive index increment (dn/dc) value. Chromatograms (reported in **SI 1**) were elaborated by OmniSEC software to calculate the Mw and polydispersity index (PDI). The Mw and the polydispersity index (PDI) of Ge and GeCh obtained are 1.27 x 10^5 (1.1) and 1.58 x 10^5 (1.9), respectively.

Sample preparation

Aqueous dispersions of GeCh were prepared by adding appropriate amounts of GeCh to water at 75°C for two hours (kept in a water bath), under magnetic stirring. Mixtures of GeCh with $ChEO_{10}$ micelles were prepared by adding appropriate amounts of $ChEO_{10}$ (from stock solutions) to GeCh dispersions. The resulting samples were stirred at room temperature overnight.

The preparation of wormlike micelles (WLM)/GeCh samples is a three-step procedure. First, solutions of concentrated WLM were prepared by stirring overnight, in the same vial, the required amount of $ChEO_{10}$ stock solution (20% w/w) with $C_{12}EO_3$ and half the total amount of H_2O. In the second step, the appropriate amount of GeCh polymer was dispersed in the remaining amount of H_2O under magnetic stirring for 2 hours at 75°C, in a water bath. Finally, the solutions of concentrated WLM were added to each vial containing the polymer dispersion (third step) and the resulting samples were stirred at room temperature overnight.

All samples were centrifuged (15 min at 6000 rpm) in order to remove trapped air bubbles due to the viscoelasticity before performing rheological measurements and SANS experiments.

All concentrations are made by weight and therefore expressed in % w/w.

Rheological measurements

Rheological experiments were performed on a controlled stress Haake RheoStress 300 Rotational Rheometer equipped with a Haake DC10 thermostat, using a cone-plate geometry (Haake CP60Ti, diameter = 60 mm; cone =1°; gap = 0.053 mm). Stress sweep measurements were carried out to assess the linear viscoelastic response range of the samples. Dynamic frequency sweeps were then performed at 20°C in the range 0.01 to 100 rad·s^{-1} by the application of a constant, small deformation ($\gamma = 0.01$) in the linear regime (as determined from the strain sweeps). Small aliquots of the gels were placed on the lower plate using a spatula. Each sample was allowed to rest for five minutes after lowering the upper plate before starting the experiment to ensure

dissipation of any pre-shearing due to loading. Most measurements were repeated three to four times and the curves shown are representative measurements.

Cryogenic Transmission Electron Microscopy (Cryo-TEM)

Cryo-TEM measurements were performed with a Zeiss TEM Libra 120 instrument (Carl Zeiss NTS, Oberkochen, Germany). The instrument was operated at 80 kV in zero-loss bright-field mode. Digital images were recorded under low dose conditions with a BioVision Pro-SM Slow Scan CCD camera system (Proscan elektronische Systeme GmbH, Germany) and iTEM software (Olympus Soft Imaging Solutions GmbH, Münster, Germany). An underfocus of 1-3 µm was used to enhance contrast. Thin films of sample solution were prepared by placing a small drop of the sample on a copper grid-supported perforated polymer film, covered with thin carbon layers on both sides. After the drop was blotted with filter paper, thin sample films (10-500 nm) spanned the holes in the polymer film. Immediately after blotting, the samples were vitrified by plunging them into liquid ethane, held just above its freezing point. Samples were kept below -165°C and protected against atmospheric conditions during both transfer to the TEM and examination.

Small-angle neutron scattering (SANS)

Measurements. Small-angle neutron scattering experiments were performed principally on the D33 instrument at the ILL (Institut Laue Langevin, Grenoble, France). Samples containing WLM and GeCh were measured in quartz Hellma cells with a 2 mm path length at 20°C; samples containing only the surfactant ($ChEO_{10}$) and the polymer were measured by using quartz cuvettes suitable for gel samples, at 25°C. On D33 instrument wavelengths between 6 and 13 Å were used with detector distances of 2 m and 12 m, to cover a *q* range between ca. 1.4×10^{-3} and 0.45 $Å^{-1}$. Samples were prepared in D_2O to optimize the contrast with the protonated surfactant and polymer. **Data analysis.** SANS data were analysed using Sasview software (3.1.2 version) [38], a Small Angle Scattering Analysis Software Package developed by the DANSE Project under NSF Award DMR-0520547.

Results and discussion

In this work, we report the formation of supramolecular networks made by the association between hydrophobically modified gellan gum, namely, gellan gum with grafted cholesterol moieties along its backbone (GeCh) and micelles of the surfactant polyoxyethylene cholesteryl ether ($ChEO_{10}$) (**Figure 1**), an unusual surfactant bearing a cholesterol tail group and a short polyethylene oxide chain (10 EO units) as the headgroup. A specificity of this work is that we explore and compare the association of GeCh with *short* micelles ($ChEO_{10}$ alone) and *long* micelles, where elongation is triggered by adding a small amount of the co-surfactant triethylene glycol monododecyl ether ($C_{12}EO_3$) to $ChEO_{10}$ [39]. In the first part, linear and non-linear rheological properties are reported; in the second part, morphological studies of the gels using small-angle neutron scattering (SANS) are discussed.

Rheological properties

Networks of gellan with small micelles of $ChEO_{10}$

Low concentration solutions of the pure surfactant $ChEO_{10}$ display a liquid-like behaviour; a 10% solution has a viscosity of only a few mPa·s [40]. Upon the addition of a small amount of GeCh (0.2%) to $ChEO_{10}$ (5%) solutions, the solution becomes shear-thinning, and shows an enhancement in viscosity values (**Figure 2A**). With a further amount of polymer (0.5%), the viscosity increases by several orders of magnitude and displays a clear shear-thinning behaviour with a Newtonian plateau and a viscosity at low shear rates of ca. 450 Pa·s (**Figure 2A**). Dynamic shear oscillatory measurements reveal a liquid-like behaviour for the pure surfactant solution (**Figure 2B**), some enhancement of the viscoelasticity with 0.2% polymer, and a predominantly solid-like viscoelastic behaviour in the presence of 0.5% GeCh, with *G'* overtaking *G"* at low frequency (ca. 0.1 rad·s^{-1}). Therefore, the addition of modified polymer induces the formation of a structured network, which gives rise to viscoelasticity. Visual inspection corroborates the existence of strong interactions between the surfactant and the polymer: solutions of GeCh alone are slightly turbid, reflecting the limited solubility of the modified polymer in water, due to the grafted hydrophobic moieties (unlike other HMPs which self-assemble into viscoelastic networks on their own [10, 11]); in the presence of $ChEO_{10}$ instead, the solutions are clear, pointing to solubilisation of the hydrophobic pendant groups by the surfactant. Given the identical nature of the hydrophobic tails of the surfactant and the pendant moieties of the polymer, a hydrophobically-driven association between the polymer and the surfactant is expected, where the grafted cholesterol groups may become solubilised within the micelles or smaller aggregates. Above a threshold polymer concentration (ca. 0.5%), these hydrophobic interactions induce the formation of a percolating network, consisting of the polymeric chains connected by micellar aggregates that act as junctions for the network. Another possibility we need to consider however is that the surfactant could simply encapsulate the hydrophobic stickers, protecting them from contact with water, without however acting as connections for the network. Based on the intrinsic viscosity of the starting polymer (*pre*-modification), the polymer is below the entanglement concentration, *C** (estimated at 1.2%), hence the onset of a solid-like behaviour cannot be attributed to polymer reptation alone, but the formation of a connected network.

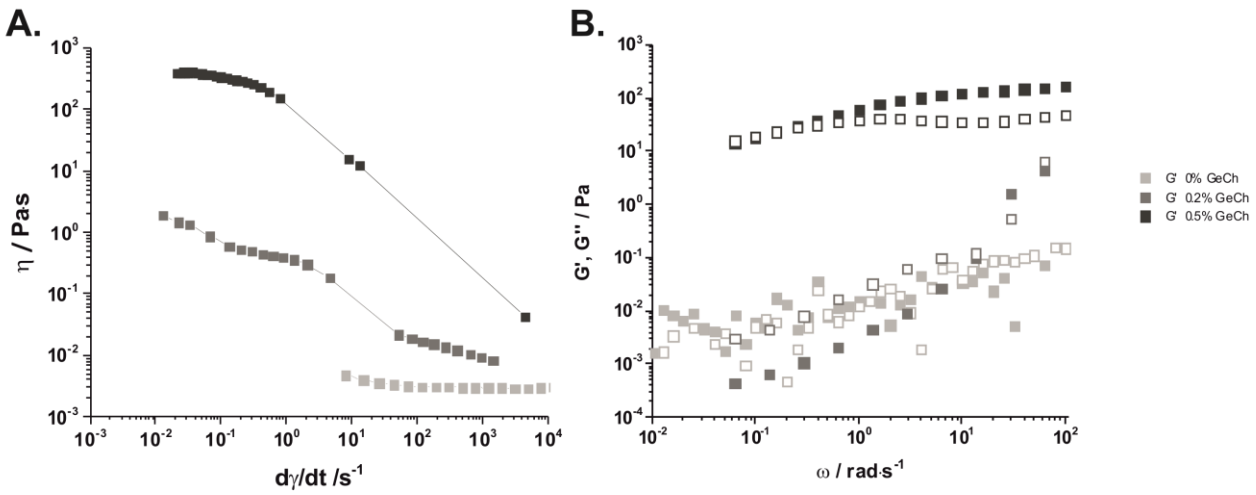

Figure 2. A. Steady state flow curves from solutions of the surfactant $ChEO_{10}$ (5%) and its mixtures with either 0.2% or 0.5% modified gellan gum, GeCh. **B**. Dynamic frequency sweeps of $ChEO_{10}$ (5%) and its mixtures with either 0.2% or 0.5% GeCh.

Next, we examine the effect of surfactant concentration on the properties of the networks. With the addition of 0.2% GeCh, the solutions are still free-flowing (but become more viscous), while the addition 0.5% GeCh to 2 - 20% surfactant leads to a predominantly solid-like response, which are able to withstand their own weight when turned upside down (**SI 1**). Frequency sweeps of $ChEO_{10}$/GeCh mixtures are shown in **Figure 3A**, at a fixed concentration of polymer (0.5%). Increasing $ChEO_{10}$ concentration from 2 to 15% w/w induces a predominantly solid-like, viscoelastic behaviour, with a gradual increase in both moduli *G'* and *G"*, and a shift of their cross-over towards lower frequencies. While the frequency sweep profile with 2% $ChEO_{10}$ is reminiscent of a Maxwell model, at higher surfactant concentrations the behaviour clearly departs from this behaviour, reflecting the existence of multiple relaxation processes: mainly, the association/dissociation of hydrophobic stickers from surfactant aggregates, and polymer reptation. The curves are remarkably similar above 2% $ChEO_{10}$ and it is possible to construct a master curve by normalising modulus and frequency by the value at the cross-over point (supplementary information, **SI 3**), as reported before [13]. The relative self-similarity of these curves is an indication that the rheological enhancement observed can be attributed to concentration effects, rather than structural reorganisations leading to additional relaxation processes [41-43]. Key parameters are summarised in **Figure 3B** (value of the elastic modulus *G'* at 10 rad·s^{-1}) and **Figure 3C** (maximum relaxation time τ_R, taken as $\tau_R = 1/\omega_c$, where ω_c is the frequency where *G'* and *G"* cross-over). With the addition of 2% $ChEO_{10}$, both moduli *G'* and *G"* increase by about one order of magnitude compared to the pure polymer suspension. Adding 5% $ChEO_{10}$ leads to another order of magnitude increase in *G'* and *G"*. However, with further addition of the surfactant (10 and 15%), the increase is less pronounced and both *G'* and τ_R stabilise at a plateau value (**Figure 3B**). This behaviour suggests a saturation of the connection sites

of the polymer. To test this hypothesis, we estimate the maximum number of possible connections, based on the number of sticker groups per chain. Considering an average M_w of 916 g/mol for the modified GeTBA unit (a tetrasaccharide composed of two glucose units, one glucuronic acid unit and one rhamnose unit, where TBA is the counterion, replaced by cholesterol at a grafting density of 20% cholesterol per Ge-TBA repeat unit), a 0.5% solution of gellan corresponds to 5.5×10^{-6} mol/g of the repeat tetrasaccharide unit, and therefore to 1.1×10^{-6} mol/g of cholesterol stickers. With 2% $ChEO_{10}$ (M_w 827 g/mol), the concentration is 2.4×10^{-5} mol/g of surfactant, i.e. a $ChEO_{10}$/sticker ratio of ca. 22:1 (molar); with 15% surfactant, this ratio becomes 166:1. There is therefore quite a large excess of surfactant, considering also that, due to topological constraints, not all pendant groups may be accessible. It is expected however that a number of surfactant molecules (more than one) are involved in the solubilisation of sticker groups to create a junction (this is confirmed by the analysis of the scattering data in the last section). Therefore, it is not surprising that increasing the surfactant concentration beyond 2%, i.e. from a 22:1 surfactant:cholesterol ratio to 55:1 (5%) still leads to an enhancement of the viscoelastic properties, up to the highest concentration studied (15%), due to additional connections being made. However, at the highest concentration studied, the plateauing in the rheological parameters may indeed reflect a saturation of the sticker groups.

In summary, mixing the cholesterol-based surfactant with the modified gellan gum (0.5%) leads to the build-up of a viscoelastic network. Increasing the amount of surfactant results in the creation of additional elastically active connections, increasing both the storage modulus and the relaxation time; however, at 15% surfactant, a saturation of the elastic properties is reached.

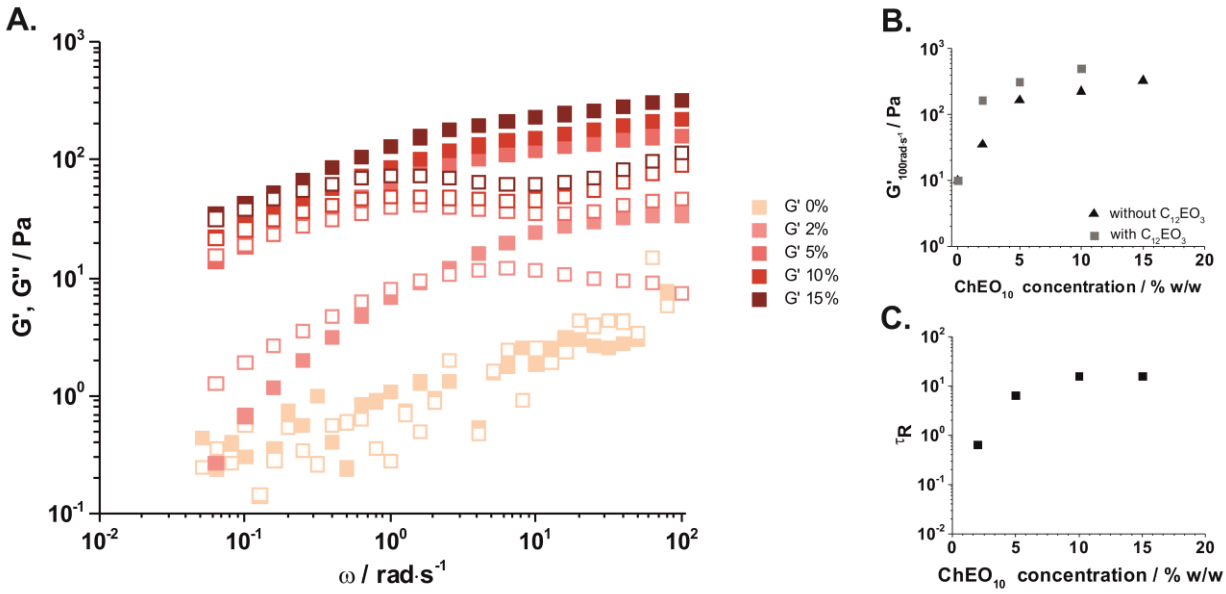

Figure 3. A. Frequency sweep curves of mixtures of 0.5% GeCh with increasing amounts of the surfactant $ChEO_{10}$ (0, 2, 5, 10 and 15%). **B**. *G'* values (at 100 rad·s^{-1}) for mixtures of 0.5% GeCh with increasing amounts

of $ChEO_{10}$, in the absence (black triangles) or presence (grey squares) of the co-surfactant $C_{12}EO_3$. **C.** Relaxation time τ_R for mixtures of 0.5% GeCh with $ChEO_{10}$.

Networks of gellan with long micelles ($ChEO_{10}$+$C_{12}EO_3$)

Effect of co-surfactant concentration

Next, we turn to the effect of the length of the micelles on the connectivity of the network. The addition of the small headgroup co-surfactant $C_{12}EO_3$ to solutions of $ChEO_{10}$ results in the longitudinal growth of the micelles into flexible, elongated micelles (WLM), as reported elsewhere [44] and shown by SANS [39], rheology [39] and Cryo-TEM [13]. This elongation by adding a small amount of a co-surfactant provides a convenient handle to explore the impact of the length of the connector in building the network.

The modified polymer (0.5%) was mixed to solution of WLM with varying $ChEO_{10}$/$C_{12}EO_3$ ratio (10% $ChEO_{10}$, and 0.5-1% $C_{12}EO_3$, corresponding to $ChEO_{10}$:$C_{12}EO_3$ molar ratios between 10:1 and 3.3:1). Frequency sweep curves from $ChEO_{10}$/$C_{12}EO_3$ wormlike micelle solutions are compared to the same micellar solutions mixed with the modified gellan, which we refer to as "bridged" micelles, in contrast to "naked" micelles **(Figure 4)**. All naked WLM solutions at increasing $C_{12}EO_3$/$ChEO_{10}$ ratios show a predominantly solid-like viscoelastic behaviour, as expected for an entangled network of wormlike micelles. The addition of the polymer induces an increase in both moduli of at least one order of magnitude, at all $C_{12}EO_3$ concentrations. The values of *G'* obtained for the bridged micelles are similar at all concentrations of co-surfactant, albeit slightly lower at the highest concentration (1.5%) (**Figure 4F**, **SI 4**). At this concentration (1.5% $C_{12}EO_3$), the solutions in the absence of polymer are slightly turbid in appearance, suggesting the presence of lamellar phases, which may come from the excess of $C_{12}EO_3$. Overall, the gels obtained by mixing WLM with gellan are quite stiff, with *G'* and *G"* fairly independent of frequency and very long relaxation times (no visible cross-over in the frequency range studied). Overall, no benefit is gained by increasing the amount of co-surfactant, as all mixtures give a very comparable rheological response (**Figure 4F**). However, the response in the presence of the co-surfactant is stronger than in its absence, as shown for instance by the values of the plateau moduli (**Figure 3B**), and the very large relaxation times. This is discussed further down.

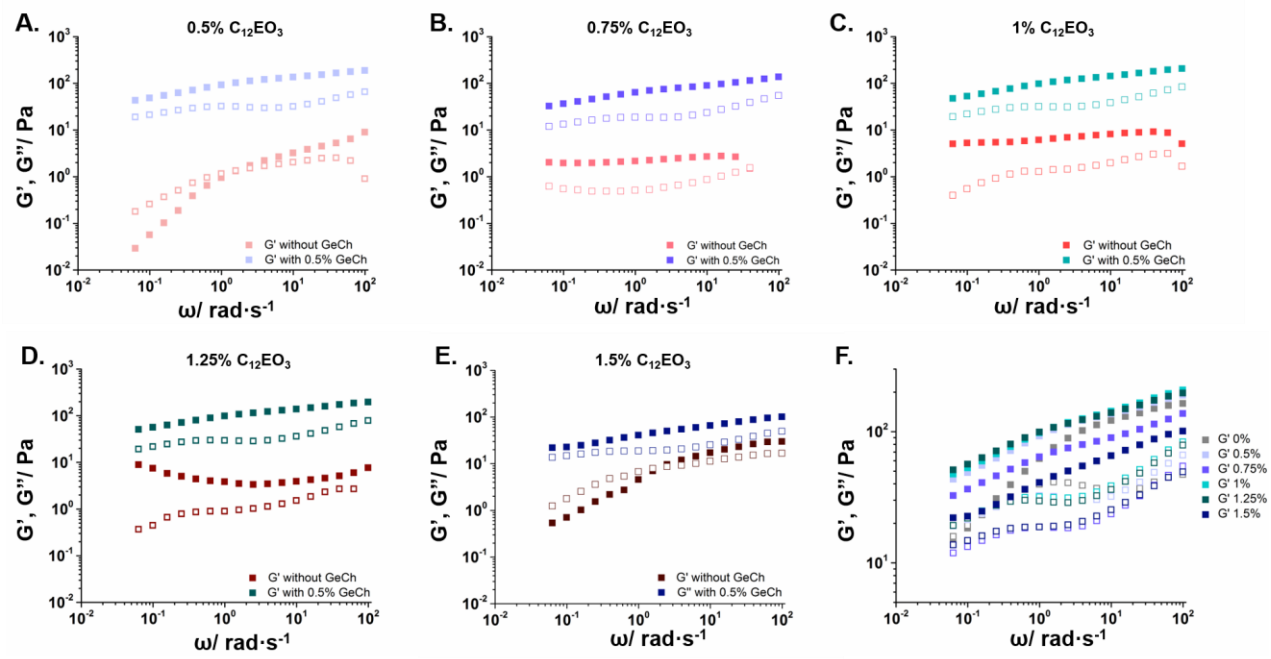

Figure 4. A. to **E**. Oscillatory shear frequency sweeps of wormlike micelles of $ChEO_{10}$ (5%) and increasing amounts of co-surfactant ($C_{12}EO_3$: 0.5 to 1.5%) and their mixtures with GeCh (0.5%). **F**. All frequency sweep curves for the polymer/WLM mixtures.

Effect of polymer concentration

We now examine the effect of varying polymer concentration at a fixed concentration of wormlike micelles (5% $ChEO_{10}$ /1% $C_{12}EO_3$) in **Figure 5A**. Increasing the amount of polymer in the mixture leads to a gradual increase in both moduli, while the shape of the frequency sweep curves remains remarkably similar, with both moduli fairly independent of frequency. At 10 rad·s^{-1}, *G'* values are: 8, 30, 70 and 240 Pa with 0, 0.1, 0.2 and 0.5% added gellan, showing that new connections for the network are created with each addition of polymer. Given the very large excess of $ChEO_{10}$ surfactant with respect to the number of cholesterol stickers (see calculation above), it is not surprising that the introduction of new pendant groups leads to new connections, since there is an excess of surfactant. The plateau modulus G_0 and the number of effective or active elastic chains, ν_{eff}, are related by [45]:

$$G_0 = \nu_{eff} RT \qquad \text{Equation 1}$$

where R is the universal gas constant and T the temperature. From this relationship, it is possible to estimate a mesh size, ξ, with $\xi = \sqrt[3]{1/\nu_{eff}}$. Taking the value of *G'* at 40 rad·s^{-1} as the plateau value, we obtain the following mesh sizes: 763, 504, 353 and 241 Å^3 for 0, 0.1, 0.2 and 0.5% polymer (this value varies by up to 5% when taking the value of *G'* at 100 rad/s). By estimating the number of sticker groups available (as described above), we find that the number of new junctions created at each incremental addition of polymer (from 0 to 0.1%, 0.1% to 0.2% etc) is comparable, albeit slightly lower (by a factor of 15 to 25) to the number of stickers added. Namely, with each increment of polymer, 5.6×10^{15}, 1.5×10^{16}, and 4.8×10^{16} new junctions are created (per cm^3), while 1.3×10^{17}, 2.6×10^{17}, and 6.6×10^{17} grafted cholesterol groups are added. Given the

fact that not all stickers are expected to contribute, either because of topological constraints, or because they do not create elastically active chains, these numbers are in remarkable good agreement. Since there is a large excess of surfactant (ca. 55:1 surfactant:sticker at 5% $ChEO_{10}$ and 0.5% GeCh; 277:1 with 0.1% polymer), it is therefore not surprising that gradually increasing polymer concentration leads to increased elasticity; this increase in elasticity is compatible with a large proportion of the pendant groups contributing to the connectivity.

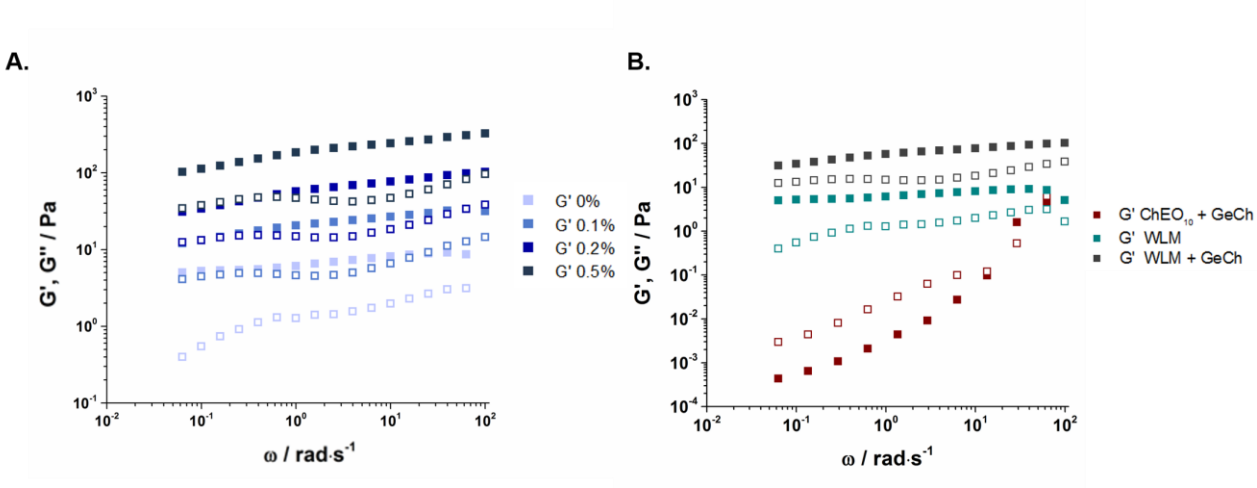

Figure 5. A. Oscillatory shear frequency sweeps of wormlike micelles of $ChEO_{10}$ and $C_{12}EO_3$, at a fixed concentration and ratio (5%:1%) mixed with increasing amounts of GeCh (0, 0.1, 0.2, 0.5%). **B.** Oscillatory shear frequency sweeps comparing the addition of modified gellan (GeCh, 0.2%) to either: $ChEO_{10}$ (5%) *short* micelles or $ChEO_{10}$:$C_{12}EO_3$ (5%:1%) *long* (wormlike) micelles. Frequency sweeps for the wormlike micelles at the same composition are also shown.

Effect of micellar length

Both *small* and *long* micelles form elastic networks when mixed with the modified gellan. The next question to ask is how the length of the connectors affects the networks. The answer is not straightforward, since the wormlike micelle solutions form an entangled network on their own, thus also displaying a solid-like viscoelastic response in the absence of polymer. In mixtures with the modified polymer, the elasticity likely results from a number of processes: the wormlike micelles relaxation (reptation, breaking and re-forming), the association and break-up of elastic connections between sticker groups and micelles, and the polymer reptation itself; it is therefore far from trivial to decouple all these effects, in particular because the length of the micelles may also be affected by the presence of the polymer, as suggested in our previous study [13]. Let us however compare the networks obtained with the same amount of polymer, 0.2% GeCh (**Figure 5B)**, mixed with either *short* ($ChEO_{10}$ only) or *long* ($ChE_{10}/C_{12}EO_3$) micelles. As described above (**Figure 2**), with the short micelles, at 5% $ChEO_{10}$, the connections are insufficient to induce the formation of a strong network, and the rheological response is quite weak. However, with the same amount of $ChEO_{10}$ but doped with $C_{12}EO_3$, thus longer

micelles (5%$ChEO_{10}$/1%$C_{12}EO_3$ WLM), a strong gel-like behaviour is obtained, with a substantial enhancement of both moduli compared to the naked WLM. Therefore, data from **Figure 5B** indicate that a low amount of modified gellan gum can be connected by *long* micelles, while the same amount of shorter micelles is insufficient to form a strongly connected network, suggesting that longer micelles may be more efficient in connecting the pendant groups from the polymer.

The effect of length is also explored in **Figure 6** where a fixed amount of GeCh (0.5%) is mixed with the same concentration of $ChEO_{10}$ (2%, 5% and 10%), with and without $C_{12}EO_3$ at a fixed $ChEO_{10}/C_{12}EO_3$ ratio (i.e. short micelles vs long micelles). Rheology traces with the long micelles ($ChEO_{10}/C_{12}EO_3$) are consistently higher than the short micelles. The higher *G'* values reflect a higher density of connections, but even more striking perhaps is the absence of a crossover point between *G'* and *G"* in the range of frequencies measured: the addition of the modified polymer to WLM leads to very long relaxation times, of the order of minutes or hours (in contrast to the short micelles, where a cross-over is always observed). From a practical viewpoint, these results show that adding a small amount of co-surfactant to $ChEO_{10}$ micelles (e.g. 0.4% $C_{12}EO_3$ to 2% $ChEO_{10}$ solutions) is a very effective way of achieving stiffer gels. The very long relaxation times obtained with the wormlike micelles can probably be explained by the slower micellar dynamics (compared to the short micelles), leading to longer hydrophobic junction lifetimes. The higher density of connections may be attributed to the possibility that the same micelle connects in several points along its length, joining several polymer chains, thus leading to a range of relaxation processes, both from the polymer and the micelles.

Figure 6D shows the effect of concentration at a fixed $ChEO_{10}/C_{12}EO_3$ ratio. As for the short micelles (in **Figure 3A**), increasing the amount of surfactant, for a fixed density of cholesterol stickers, leads to increasing connectivity. As for the shorter micelles however, a plateau is reached at the highest concentration of surfactant (**Figure 3B**), suggesting that the hydrophobic pendant groups become saturated, or that topological constraints limit the number of junctions possible.

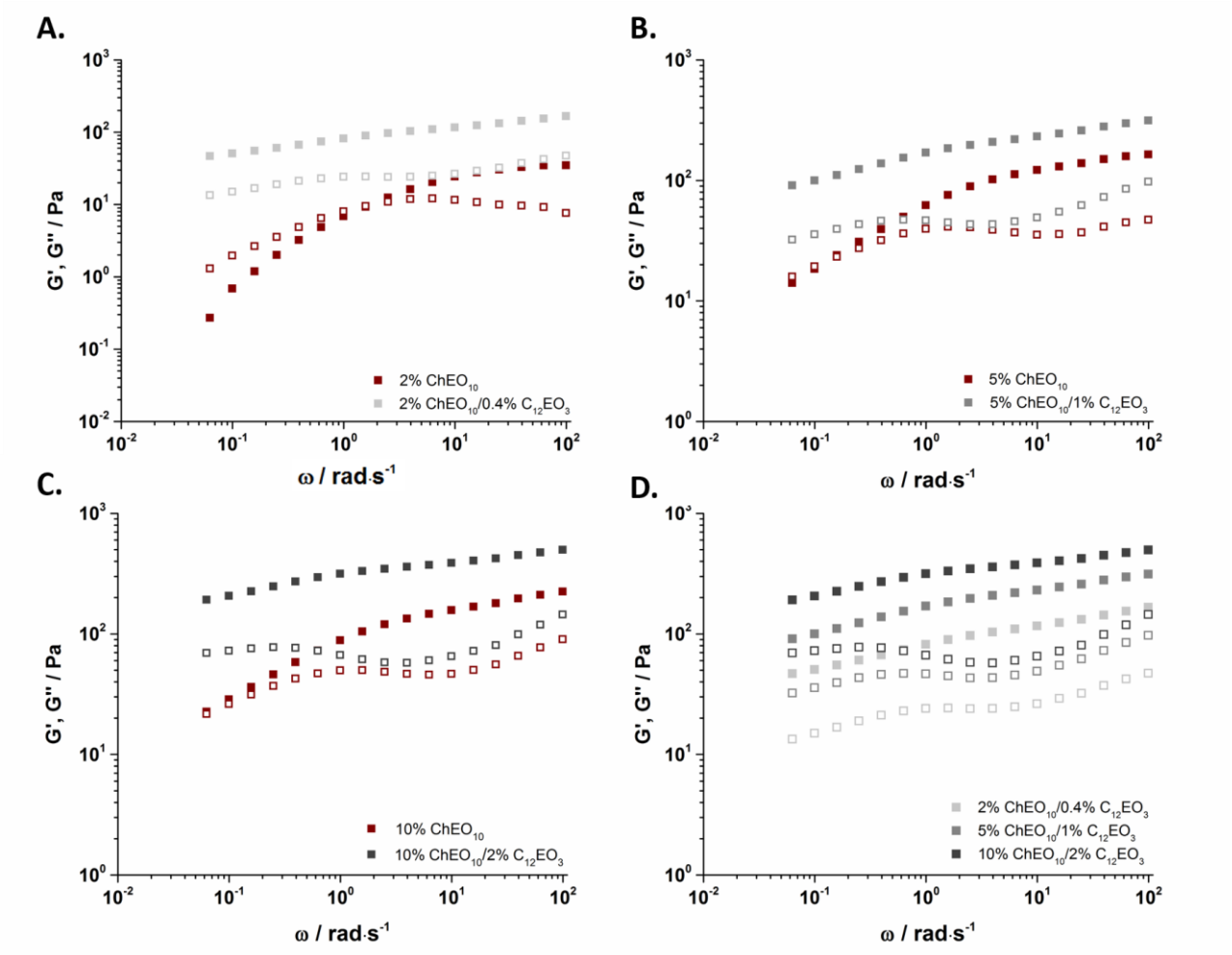

Figure 6. Frequency sweep curves comparing the addition of GeCh (0.5%) to either micelles of pure $ChEO_{10}$ (2%, 5% and 10%) or wormlike micelles at the same concentration of $ChEO_{10}$ and fixed $ChEO_{10}$:$C_{12}EO_3$ ratio (5:1 w/w). Panel **D** compares the mixtures of GeCh with wormlike micelles at varying $ChEO_{10}$ concentrations (2%, 5% and 10%) and fixed $ChEO_{10}$:$C_{12}EO_3$ ratio.

Overall, the rheological study shows that mixing the modified gellan with either short or long micelles induces the formation of a connected network. A high affinity between the modified polymer and the surfactant was expected because of the identical hydrophobic cholesterol moieties of the surfactant and the polymer. The increased density of junctions obtained by either increasing polymer or surfactant concentration suggests that the network is formed by sticker/surfactant junctions connecting polymer chains. With the longer micelles, the higher elasticity and relaxation of the network likely arises from the connectivity provided by longer micelles, which also contribute to slower dynamics.

Structural characterisation by small-angle neutron scattering measurements (SANS)

In order to assess the morphology of the self-assembled systems that underlie the solid-like rheological response, SANS measurements were conducted on mixtures of gellan with $ChEO_{10}$ micelles. Micelles of

$ChEO_{10}$ have previously been described as short rods [46], or rods with an elliptical cross-section [39]. More recent Cryo-TEM measurements [47] have revealed that the micelles are disc-like rather than cylindrical. **Figure 7** shows a representative sample, revealing in the left part of the image discs in "face-view" (very thin film) and towards the right part of the image, where the film is thicker, the discs are packing up in "edge-view", where they have a much higher contrast, due to the electrons having a longer way to travel through the material and scatter. The disc morphology is also corroborated by cryo-TEM studies on $ChEO_{10}$ aggregates from the group of Danino [48, 49], which show disc-like aggregates that transition into elongated ribbon structures at higher concentrations. The discs have a diameter of 15 – 20 nm (**Figure 7**), a dimension which agrees with the length of the rods previously reported [39, 46]. Based on the cryo-TEM study by Danino and co-workers, it is also suggested that the elongated micelles observed in mixtures with $C_{12}EO_3$ [49], or obtained with increasing concentrations of $ChEO_{10}$ [48], are ribbon-like (flat cross-section), rather than the classic spherical (or elliptical) cross-section found in wormlike micelles. The unusual packing of this surfactant is not surprising given its unconventional tail group made of a bulky steroid motif, which may more favourably pack flat, rather than into spherical assemblies. In the present work, based on Cryo-TEM evidence, SANS data were thus fitted by considering a model of flat core-shell cylinders, taking into account a corona made-up of the PEG headgroups.

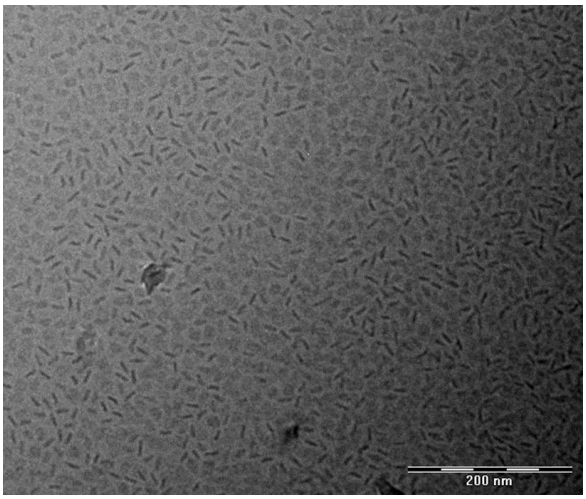

Figure 7. Cryo-TEM image showing disc-shaped aggregates in dilute (1%) solutions of $ChEO_{10}$.

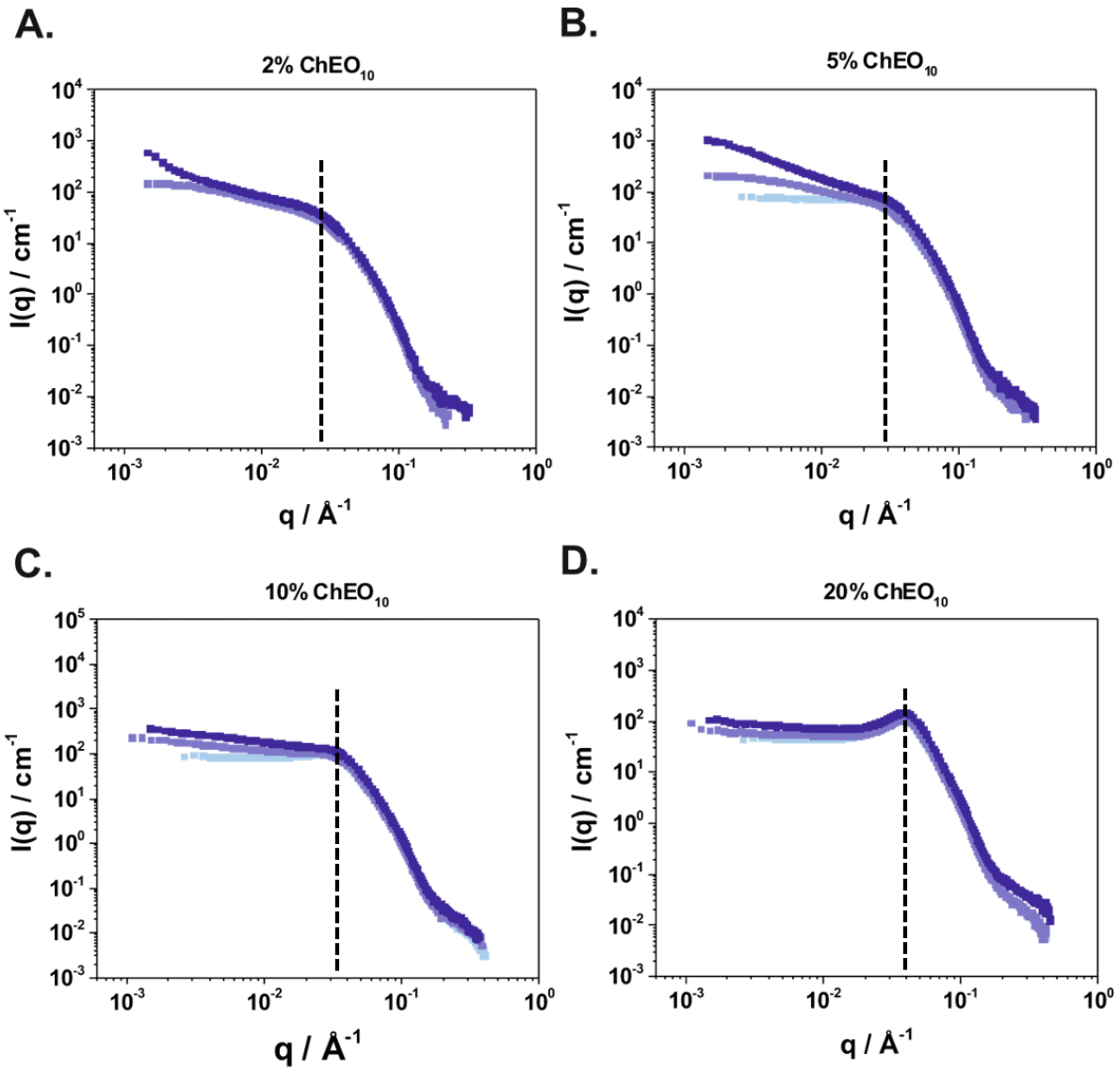

Figure 8. SANS curves from $ChEO_{10}$ micellar solutions in the absence of polymer (light shade, 5, 10 and 20%) and their mixtures with either 0.2% or 0.5 % of GeCh (increasing dark shade) at 2%, 5%, 10% and 20% $ChEO_{10}$. The vertical dotted line denotes the position of the peak.

Figure 8 shows the scattering curves obtained from pure surfactant micelles over a range of concentrations, either alone (5, 10 and 20%) or in mixtures (at 2, 5, 10 and 20%) with GeCh at 0.2 or 0.5%. At each surfactant concentration, the scattering curves overlay remarkably well, independently of the amount of polymer (0, 0.2% or 0.5%), suggesting that the scattering arises mainly from the micelles, which may be bridged by the polymer. The scattering from the polymer alone at 0.2% and 0.5% (shown in **SI 5**) shows no similarity with the patterns obtained from the mixtures. The curves can be fitted either by a fractal model, with a fractal dimension of ~2.6, or with a "gel model" [38], which reflects fluctuations on two length scales, described by a Guinier function and a Lorentzian (model described in **SI 5**). Both are compatible with the presence of polymer aggregates of various dimensions extending over very large length scales (the solutions are turbid, reflecting limited solubility, due to the cholesterol pendant groups). The scattering from the micelles and their mixtures with the

polymer (**Figure 8**) is typical of finite objects dominated by interactions that become stronger as the concentration of surfactant increases, as reflected by the presence of a structural peak in the SANS curves. The peak position shifts slightly towards the high *q*-region with higher polymer concentration and becomes more pronounced, reflecting closer inter-micellar distances. In the presence of polymer, some excess scattering becomes visible at low *q*, which increases gradually with GeCh concentration, and could either originate from the polymer itself, or from attractive interactions between the micelles connected by polymer chains; this scattering at low *q* is less pronounced at the highest micellar concentration (20%). This is discussed in more detail later with the SANS data analysis.

The scattering from $ChEO_{10}$ micelles alone (**Figure 9A**) was fitted with a (flat) core-shell cylinder model for the form factor and a hard sphere potential for the structure factor. The best parameters are summarized in **Table 1**, where the geometrical dimensions of the micelles were kept constant and the only parameter varied was the volume fraction of the (hydrated) micelles, ϕ. The micelles can be reasonably described as discs of 140 Å diameter and 38 Å thickness, with a polydispersity of the radius and length fixed at 0.12. These discs are surrounded by an EO layer of 14 Å, containing a high amount (65%) of water, as deduced from the value of the scattering length density, ρ_{shell}. This hydration value is consistent with the volume fraction of the hydrated micelles returned by the fits. The aggregation number, N_{agg}, estimated from the volume of the hydrophobic core of the micelles and the molecular volume of a cholesterol molecule (600 $Å^3$) is close to 30. The experimental curve at 2% was not measured and the curve shown in **Figure 9** is the model scattering calculated by considering a volume fraction of 3.2% hydrated micelles.

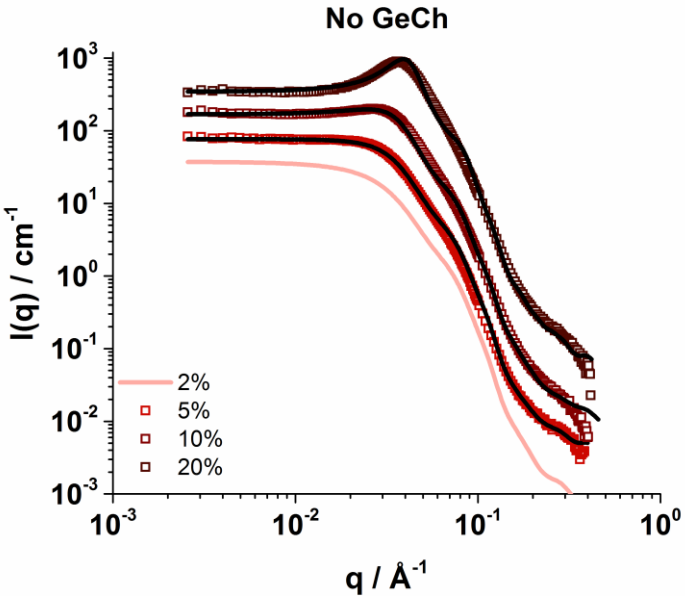

Figure 9. SANS curves from $ChEO_{10}$ micelles (5%, 10% and 20%) with solid lines showing fits to the core-shell cylinder model combined with a hard-sphere structure factor described in the text. The curve for 2% $ChEO_{10}$ micelles is calculated. Curves are staggered for better visualisation.

Table 1: SANS data parameters obtained from the analysis of the scattering curves of $ChEO_{10}$ micelles, using a combination of a core-shell cylinder and a hard-sphere structure factor. R_c is the radius of the cylinders, e_{shell} the thickness of the shell, L the length of the cylinders, ρ_c, ρ_{shell} and ρ_{D2O} the scattering length density of the core, shell, and D_2O, respectively, and Φ the volume fraction of the hydrated micelles.

Concentration of $ChEO_{10}$ (wt %)	**5%**	**10%**	**20%**
R_c **(Å)**	70	70	65
e_{shell} **(Å)**	14	14	14
L **(Å)**	38	38	38
ρ_c **c (Å^{-2})**	0.22×10^{-6}	0.22×10^{-6}	0.22×10^{-6}
ρ_{shell} **(Å^{-2})**	4.75×10^{-6}	4.75×10^{-6}	4.9×10^{-6}
ρ_{D2O} **(Å^{-2})**	6.4×10^{-6}	6.4×10^{-6}	6.4×10^{-6}
ϕ	0.08	0.16	0.30

As discussed in the previous section, the addition of modified gellan to solutions of $ChEO_{10}$ micelles leads to a small increase in viscoelasticity at 0.2% GeCh (**Figure 2B**), while gels are formed at 0.5% GeCh (**Figure 2B**, **Figure 3, SI 2**).

In the presence of modified gellan gum, the scattering curves are superimposed with the scattering from the pure micelles at large q, an indication that the size and shape of the micelles are not modified by gellan gum (**Figure 8**). However, an increase of the scattering at low q is observed, which suggests the local formation of larger structures (more limited at the highest surfactant concentration).

The data analysis was performed by considering that the organization of a fraction of the micelles f is affected by the presence of the gellan gum and leads to the formation of clusters with a finite size and fractal dimension d_f. The remaining fraction of the micelles (1-f) is not affected by the presence of gellan and is fitted by considering a hard-sphere (HS) structure factor, $S_{HS}(q)$. The cross-correlation term in the structure factor is neglected in this model.

$$I(q) = \phi f \, P(q) S_{HS}(q) + \phi(1-f) P(q) S_{agg}(q) \qquad \text{Equation 2}$$

$$S_{agg}(q) = 1 + sin\left[\left(d_f - 1\right) atan(q\xi)\right] \frac{C\Gamma(d_f-1)\xi^{d_f}}{q\xi} \frac{1}{[1+(q\xi)^2]^{\left(d_f-1\right)/2}} \qquad \text{Equation 3}$$

where C is a constant, $S_{agg}(q)$ is the fractal structure factor with a characteristic size ξ and a fractal dimension d_f as developed by Freltoft et al [50] and Teixeira [51]. $P(q)$ and $S_{HS}(q)$ are the form factor and hard sphere structure factor for the micelles, respectively, and ϕ is the total volume fraction of the micelles.

The resulting fits are shown in **Figure 10A** for 0.2% GeCh and **10B** for 0.5% GeCh.

For the highest surfactant concentration at 20%, the scattering from the micelles is almost not modified by the presence of gellan (see **Figure 8**). Only a small increase of the intensity at the lowest scattering vector is

observed, which cannot be fitted with the combined structure factors (Equation 2). For this system only, the scattering curves were suitably described by a core-shell cylinder model combined to a HS structure factor only.

The data parameters used to model the data are summarized in **Table 2**. The fractal dimension of 2.7 is also in very good agreement with the one determined for the gel without the micelles (supplementary information, **SI 6**). The values of the correlation lengths must be taken with some caution, the relative error on this parameter being relatively high (ca. 10-20%), but it remains of the order of the correlation length from the rheology measurements discussed in the previous section and also shown in **Figure 11**. An alternative model was also found to give good fits to the scattering curves, which assigned a sticky hard-sphere, or square-well potential, to a fraction of the micelles. Both models, while different, are compatible in that they describe an attractive interaction induced by the presence of the polymer, which leads to micellar clustering. The interaction is reduced (and the clusters negligible) at the highest surfactant concentration (20 %), which corresponds to a full saturation of the sticker groups.

Table 2. SANS data parameters obtained from modeling data from the $ChEO_{10}$ micelles in the presence of 0.2% and 0.5% GeCh, using a combination of a core-shell cylinder for the form factor and a square-well and hard-sphere structure factor. R_c is the radius of the cylinders, e_{shell} the thickness of the shell, L the length of the cylinders, ρ_c, ρ_{shell} and ρ_{D2O} the scattering length density of the core, shell, and D_2O, respectively, and $\phi_{micelle}$ and ϕ_{gellan} the volume fraction of micelles and gellan, respectively, f the fraction of micelles affected by gellan (as described in Equation 2).

Concentration of $ChEO_{10}$ (wt %)	**2%**		**5%**		**10%**		**20%**	
ϕ_{gellan}	**0.2**	**0.5**	**0.2**	**0.5**	**0.2**	**0.5**	**0.2**	**0.5**
R_c (Å)	70		70		70		70	
e_{shell} (Å)	14		14		14		14	
L (Å)	38		38		38		38	
ρ_c (Å^2)	0.22×10^{-6}		0.22×10^{-6}		0.22×10^{-6}		0.22×10^{-6}	
ρ_{shell} (Å^2)	4.75×10^{-6}		4.75×10^{-6}		4.75×10^{-6}		4.75×10^{-6}	
ρ_{D2O} (Å^2)	6.4×10^{-6}		6.4×10^{-6}		6.4×10^{-6}		6.4×10^{-6}	
$\phi_{micelle}$	0.032	0.035	0.08	0.1	0.16	0.17	0.32	0.37
f	1	1	0.4	0.1	0.2	0.1	0	0
ξ (Å)	160	200	160	250	160	120	-	-
d_f	2.7	2.7	2.7	2.7	2.7	2.7	-	-
C (Å^{-1})	0.45	0.6	0.7	16	4	5.5		

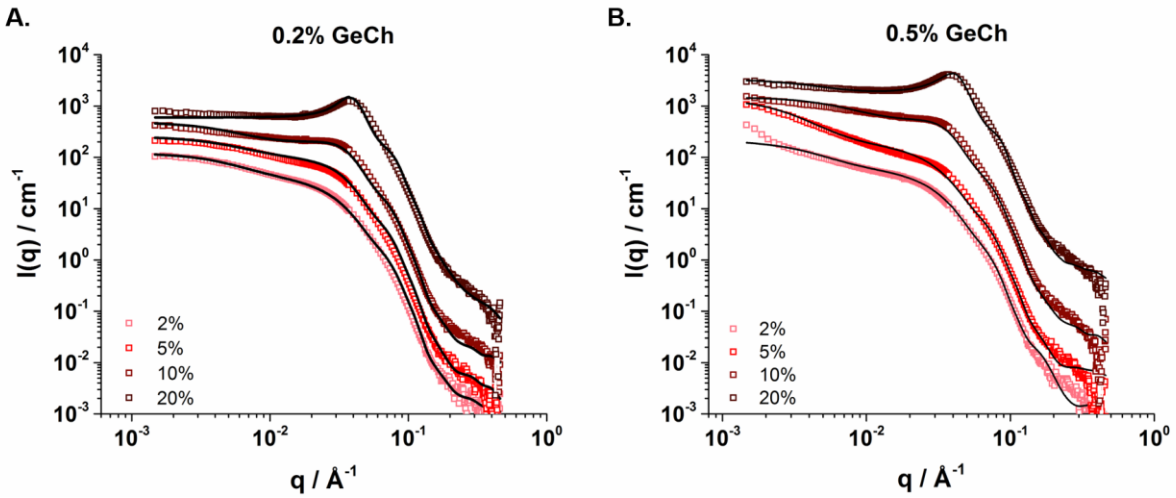

Figure 10. SANS curves from mixtures of $ChEO_{10}$ micelles (2%, 5%, 10% and 20%) with modified gellan gum at: **A.** 0.2% GeCh and **B.** 0.5% GeCh. Solid lines are fits to the core-shell cylinder model (describing the micelles) interacting thorugh a hard-sphere structure factor, and an added contribution from fractal aggregates, as described in the text. Curves are staggered for better visualisation.

The position of the peak in the data sets with 0.5% gellan (**Figure 10B**) was used to extract a typical length scale or periodicity in the gels, corresponding to $d = 2\pi/q_{peak}$, which is compared in **Figure 11** with the values of the mesh size estimated from the plateau modulus, G_0, in shear oscillatory measurements (Equation 1, **Figure 3B**). The mesh size obtained from the two approaches are in good agreement and are also in reasonable agreement with the best parameter fit values (Table 2).

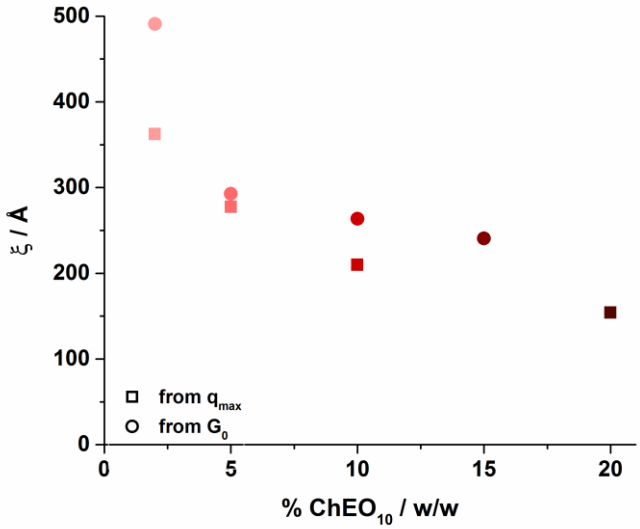

Figure 11. Mesh size obtained of the gels made by 0.5% GeCh with increasing concentrations of micelles obtained either from the peak position q_{max} in the SANS curves or the value of the plateau modulus G_0 from shear oscillatory rheology.

Conclusion

In this study, the association between a hydrophobically modified polysaccharide, gellan gum, with micelles based on a surfactant bearing the same hydrophobic tail as the pendant groups was investigated. More specifically, gellan gum was modified by grafting cholesterol groups, and mixed with polyoxyethylene cholesteryl ether ($ChEO_{10}$), which comprises a cholesterol tail group linked to a small polyoxyethylene headgroup. The effect of composition (polymer and surfactant concentration) as well as micellar morphology, were studied, the latter by doping $ChEO_{10}$ micelles with a small headgroup co-surfactant, which drives their elongation into wormlike micelles. We found that associative interactions between the surfactant micelles and the modified polymer lead to the formation of a percolating network above a threshold concentration of polymer (ca. 0.5%), and the shear elastic modulus can be tuned by increasing surfactant concentration, however saturation of binding sites is reached and not much improvement in the properties occurs beyond ca. 15% $ChEO_{10}$. With the long micelles, oscillatory rheology measurements reveal a predominantly solid-like behaviour, with no cross-over between *G'* and *G"*, reflecting very large relaxation times, of the order of minutes or hours, likely arising from the improved connectivity provided by longer micelles, which also contribute to slower dynamics. From a practical viewpoint, our results show that adding a small amount of co-surfactant to $ChEO_{10}$ micelles to drive wormlike micelle formation is an effective way of achieving stiffer gels. The morphology of the gels was studied by small-angle neutron scattering measurements. $ChEO_{10}$ micelles show an unusual disc morphology (attributed to the flat, bulky steroid skeleton) with a 140 Å diameter (cholesterol core) and a hydrated PEO corona of 38 Å thickness, and interact through a hard-sphere potential. Upon addition of the polymer, the scattering pattern is only mildly affected, with the micelles still dominating the scattering, while excess scattering became visible at low q. Data analysis confirms that the size and shape of the micelles are not modified by the presence of gellan gum but their spatial arrangement is slightly modified: the polymer induces the formation of small micellar clusters, which are at the origin of the increase in scattering at low q. The scattering data therefore confirm that the onset of gelation is due to surfactant micelles acting as junction points for the network.

Overall, this work provides detailed structural insights into a network constituted by polymeric chains connected by micellar aggregates, through hydrophobic interactions between the cholesterol cores of the micelles and the cholesterol moieties grafted along the polysaccharide backbone. These associative gels, based on a vastly abundant polysaccharide, provide a simple strategy towards building functional hydrogels based on materials from renewable sources.

Acknowledgements

The ILL is acknowledged for the provision of neutron beam time (9-10-1447) [52]. NZ acknowledges the financial support from Sapienza, University of Rome (grant no. RM11715C1743EE89 is acknowledged). Jonny Eriksson is thanked for the Cryo-TEM measurements.

This work benefited from the use of the SasView application, originally developed under NSF award DMR-0520547. SasView contains code developed with funding from the European Union's Horizon 2020 research and innovation programme under the SINE2020 project, grant agreement No 654000.

References

[1] Webber, M. J., Appel, E. A., Meijer, E. W., and Langer, R.; *Nature materials*, *15*(1), 2016, 13.

[2] Tan, C. S. Y., Liu, J., Groombridge, A. S., Barrow, S. J., Dreiss, C. A., and Scherman, O. A.; *Advanced Functional Materials*, *28*(7), 2018, 1702994.

[3] Serres-Gómez, M., González-Gaitano, G., Kaldybekov, D. B., Mansfield, E. D., Khutoryanskiy, V. V., Isasi, J. R., and Dreiss, C. A.; *Langmuir*, *34*(36), 2018, 10591-10602.

[4] Annable, T., Buscall, R., Ettelaie, R., and Whittlestone, D.; *Journal of Rheology*, *37*(4), 1993, 695-726.

[5] Tixier, T., Tabuteau, H., Carriere, A., Ramos, L., and Ligoure, C.; *Soft Matter*, *6*(12), 2010, 2699-2707.

[6] Lodge, T. P., Taribagil, R., Yoshida, T., and Hillmyer, M. A.; *Macromolecules*, *40*(13), 2007, 4728-4731.

[7] Cabane, B., Lindell, K., Engström, S., and Lindman, B.; *Macromolecules*, *29*(9), 1996, 3188-3197.

[8] Nilsson, S., Thuresson, K., Hansson, P., and Lindman, B.; *The Journal of Physical Chemistry B*, *102*(37), 1998, 7099-7105.

[9] Karlson, L., Joabsson, F., and Thuresson, K.; *Carbohydrate polymers*, *41*(1), 2000, 25-35.

[10] Couillet, I., Hughes, T., Maitland, G., and Candau, F.; *Macromolecules*, *38*(12), 2005, 5271-5282.

[11] Talwar, S., Scanu, L., Raghavan, S. R., and Khan, S. A.; *Langmuir*, *24*(15), 2008, 7797-7802.

[12] Alves, L., Lindman, B., Klotz, B., Böttcher, A., Haake, H. M., and Antunes, F. E.; *Journal of colloid and interface science*, *513*, (2018), 489-496.

[13] Afifi, H., da Silva, M. A., Nouvel, C., Six, J. L., Ligoure, C., and Dreiss, C. A.; *Soft Matter*, *7*(10), 2011, 4888-4899.

[14] Glass, J. E., Polymers in aqueous media: performance through association, advances in chemistry series 223, American Society, Washington, 1989

[15] Iohara, D., Okubo, M., Anraku, M., Uramatsu, S., Shimamoto, T., Uekama, K., and Hirayama, F.; *Molecular pharmaceutics*, *14*(8), 2017, 2740-2748.

[16] Dowling, M. B., Kumar, R., Keibler, M. A., Hess, J. R., Bochicchio, G. V., and Raghavan, S. R.; *Biomaterials*, *32*(13), 3351-3357.

[17] Knöös, P., Wahlgren, M., Topgaard, D., Ulvenlund, S., and Piculell, L.; *The Journal of Physical Chemistry B*, *118*(32), 2014, 9757-9767.

[18] Can, V., Kochovski, Z., Reiter, V., Severin, N., Siebenbürger, M., Kent, B., Just, J., Rabe J., P., Ballauff, M., and Okay, O.; *Macromolecules*, *49*(6), 2016, 2281-2287.

[19] Kronberg, B., Holmberg, K., and Lindman B., Surfactant–polymer systems. In *Surface Chemistry of Surfactants and Polymers*, John Wiley and Sons, Ltd., 2014.

[20] Piculell, L., Thuresson, K., and Lindman, B.; *Polymers for advanced technologies*, *12*(1-2), 2001, 44-69.

[21] Molchanov, V. S., and Philippova, O. E.; *Journal of colloid and interface science*, *394*, 2013, 353-359.

[22] Dreiss, C. A.; *Soft Matter*, *3*(8), 2007, 956-970.

[23] Dreiss, C. A., and Feng, Y. Wormlike Micelles: Advances in Systems, Characterisation and Applications. Royal Society of Chemistry, 2017.

[24] Ramos, L., and Ligoure, C.; *Macromolecules*, *40*(4), 2007, 1248-1251.

[25] Akay, G., Hassan-Raeisi, A., Tuncaboylu, D. C., Orakdogen, N., Abdurrahmanoglu, S., Oppermann, W., and Okay, O.; *Soft Matter*, *9*(7), 2013, 2254-2261.

[26] Matricardi, P., Cencetti, C., Ria, R., Alhaique, F., and Coviello, T.; *Molecules*, *14*(9), 2009, 3376-3391.

[27] Mahajan, H. S., and Gattani, S. G.; *Chemical and Pharmaceutical Bulletin*, *57*(4), 2009, 388-392.

[28] D'Arrigo, G., Di Meo, C., Gaucci, E., Chichiarelli, S., Coviello, T., Capitani, D., Alhaique, F., and Matricardi, P.; *Soft Matter*, *8*(45), 2012, 11557-11564.

[29] Morris, E. R., Nishinari, K., and Rinaudo, M.; *Food Hydrocolloids*, *28*(2), 2012, 373-411.

[30] Singh, B. N., Trombetta, L. D., and Kim, K. H.; *Pharmaceutical development and technology*, *9*(4), 2005, 399-407.

[31] Oliveira, J. T., Martins, L., Picciochi, R., Malafaya, P. B., Sousa, R. A., Neves, N. M., Mano, J. F., and Reis, R. L.; *Journal of Biomedical Materials Research Part A*, *93*(3), 2010, 852-863.

[32] Grasdalen, H., and Smidsrød, O.; *Carbohydrate polymers*, *7*(5), 1987, 371-393.

[33] Osmałek, T., Froelich, A., and Tasarek, S.; *International journal of pharmaceutics*, *466*(1-2), 2014, 328-340.

[34] Cencetti, C., Bellini, D., Longinotti, C., Martinelli, A., and Matricardi, P.; *Journal of Materials Science: Materials in Medicine*, *22*(2), 2011, 263-271.

[35] Silva-Correia, J., Miranda-Gonçalves, V., Salgado, A. J., Sousa, N., Oliveira, J. M., Reis, R. M., and Reis, R. L.; *Tissue Engineering Part A*, *18*(11-12), 2012, 1203-1212.

[36] Chang, S. J., Huang, Y. T., Yang, S. C., Kuo, S. M., and Lee, M. W.; *Carbohydrate polymers*, *88*(2), 2012 684-689.

[37] Montanari, E., De Rugeriis, M. C., Di Meo, C., Censi, R., Coviello, T., Alhaique, F., and Matricardi, P.; *Journal of Materials Science: Materials in Medicine*, *26*(1), 2015, 32.

[38] https://www.sasview.org.

[39] Afifi, H., Karlsson, G., Heenan, R. K., and Dreiss, C. A.; *Journal of colloid and interface science*, *378*(1), 2012, 125-134.

[40] Afifi, H., Karlsson, G., Heenan, R. K., and Dreiss, C. A.; *Langmuir*, *27*(12), (2011), 7480-7492.

[41] Bernardes, J. S., da Silva, M. A., Piculell, L., and W. Loh, W.; *Soft Matter*, 6(1), 2010, 144–153.

[42] Piculell, L., Egermayer, M., and Sjostrom, J.; *Langmuir*, 19(9), 2003, 3643– 3649.

[43] A. Y. Malkin, Rheology Fundamentals, ChemTec Publishing, Toronto, 1994.

[44] Acharya, D. P., and Kunieda.; *The Journal of Physical Chemistry B*, *107*(37), 2003, 10168-10175.

[45] Green, M. S., and Tobolsky, A. V.; *The Journal of Chemical Physics*, *14*(2), 1946, 80-92.

[46] Moitzi, C., Freiberger, N., and Glatter, O.; *The Journal of Physical Chemistry B*, *109*(33), 2005, 16161-16168.

[47] García-Pérez, Á., da Silva, M. A., Eriksson, J., González-Gaitano, G., Valero, M., and Dreiss, C. A.; *Langmuir*, *30*(39), 2014, 11552-11562.

[48] Danino, D., Abezgauz, L., Portnaya, I., and Dan, N.; *The journal of physical chemistry letters*, *7*(8), 2016, 1434-1439.

[49] Kesselman, E., and Danino, D. Direct-imaging Cryo-transmission Electron Microscopy of Wormlike Micelles. In *Wormlike Micelles: Advances in Systems, Characterisation and Applications*. Royal Society of Chemistry, 2017, 171-192.

[50] Freltoft, T. J. K. S. K., Kjems, S. K., and Sinha, S. K .; *Physical Review B*, 33, 1986, 269-275.

[51] Teixeira, J.; Journal of Applied Crystallography, 21(6), 1988, 781-785.

[52] Dreiss, C., Gerelli, Y., Grillo, I., Harvey, R., Pabois, O., and Wilde, P.; Understanding the interfacial behaviour of bile salts to better engineer lipid emulsions. Institut Laue-Langevin (ILL) doi:10.5291/ILL-DATA.9-13-784.